Electronic Supplementary Material (ESI) for Journal of Materials Chemistry A.


Supporting Information

# Waterbomb origami tower for convertible photothermal evaporation

Xiaojie Liu, Yanpei Tian, Fangqi Chen, Ying Mu, Andrew Caratenuto, Marilyn L. Minus, and Yi Zheng*

Department of Mechanical and Industrial Engineering, Northeastern University, Boston, MA 02115, USA.

*e-mail: y.zheng@northeastern.edu

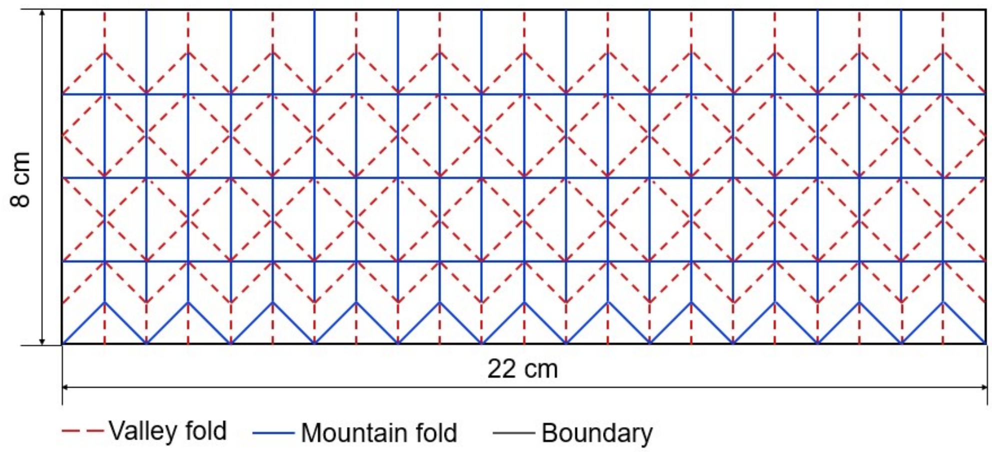


**Fig. S1.** Crease map for the origami tower.

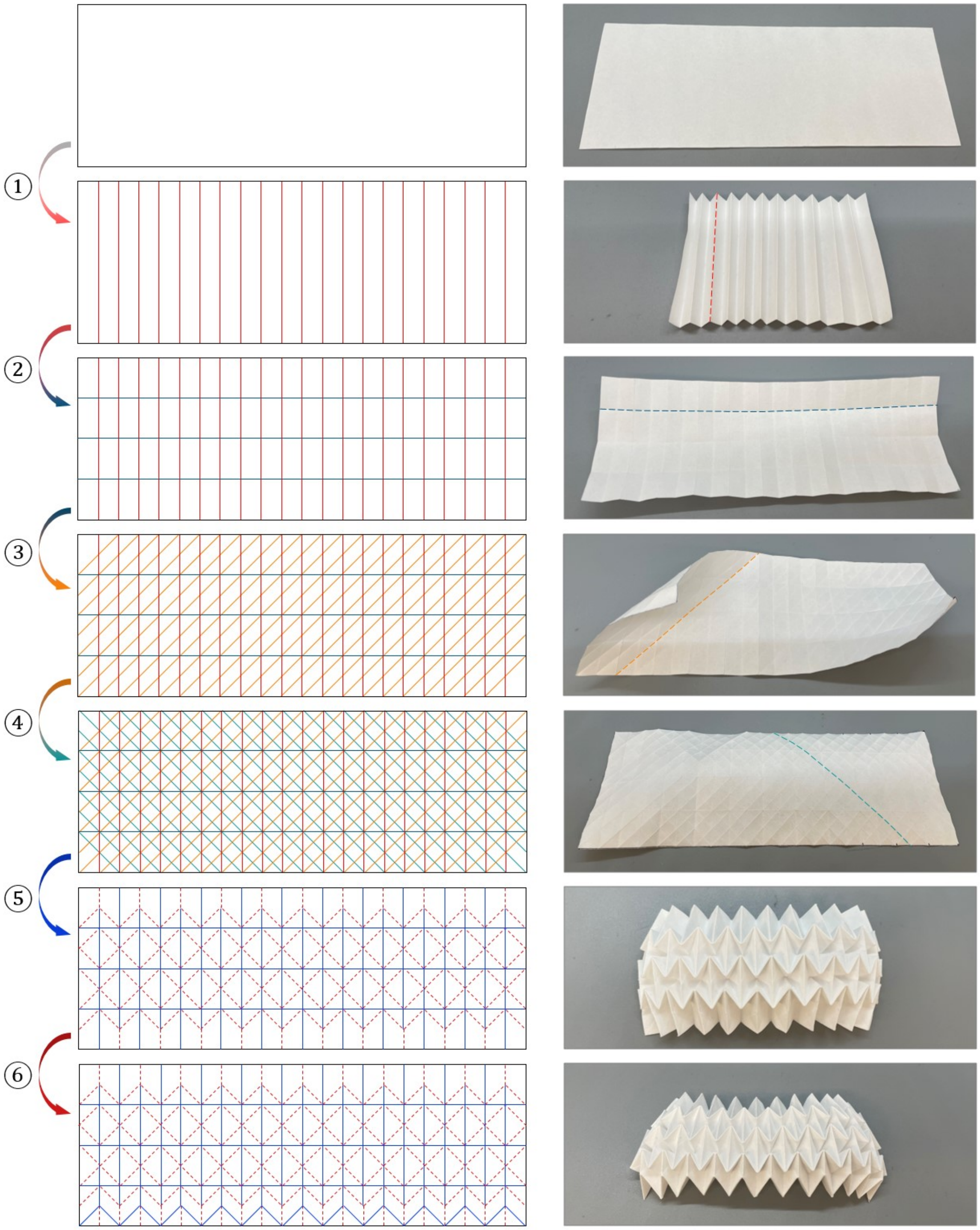


**Fig. S2.** Folding process for the origami tower step by step. The left column shows the crease map for each step, and the right column shows the photos of the folded paper corresponding to the crease map. The dashed curve on each photo represents one of the folding creases created by the corresponding step.

**Note S1**

**The folding steps for the waterbomb-patterned origami tower**

The schematic illustration of the folding process for the origami tower step by step is shown in Figure S2. The detailed corresponding description of it is shown below:

**Initial**: a cellulose paper sheet with a dimension of 22 cm in length and 8 cm in width is used for paper folding.

**Step ①**: The paper is divided into exactly 16 equal parts along the length, and the folding creases are shown in red lines. Each part is in the dimension of 1 cm × 8 cm. Note that in the steps ① - ④, the crease map does not distinguish between the valley folds and mountain folds, and it only refers to the marks created by the folding of the paper.

**Step ②**: Dividing paper into exactly 4 equal parts along the width, and the new added folding creases are shown in the dark blue lines. Each part is in the dimension of 1 cm × 2 cm.

**Step ③**: Folding diagonally as indicated by the orange lines with inclination angle of 45°.

**Step ④**: Folding diagonally as indicated by the green lines with inclination angle of 135°. So far, all of the creases needed for the origami tower are finished.

**Step ⑤**: Differentiating all the creases into the mountain folds and valley folds basing on the crease map in step ⑤. A unit waterbomb patter is in the dimension of 2 cm × 2 cm. Notice that the crease map in step ⑤ and ⑥ include the mountain and valley folds, thereinto, black line represents the boundary, blue line represents the mountain fold, and the red dashed line represents the valley fold. In the photos on the right side, we can see there are two lines of complete adjoining waterbomb patterns.

**Step ⑥**: Creating the top part of the origami tower by adding the mountain folds in the bottom line of the crease map in step ⑥. Therefore, for the 3D waterbomb-patterned structure in the photo on the right side, it is divided into top, middle, bottom, and in-water parts from the bottom up. It corresponds to the structure division of the origami tower in the manuscript.

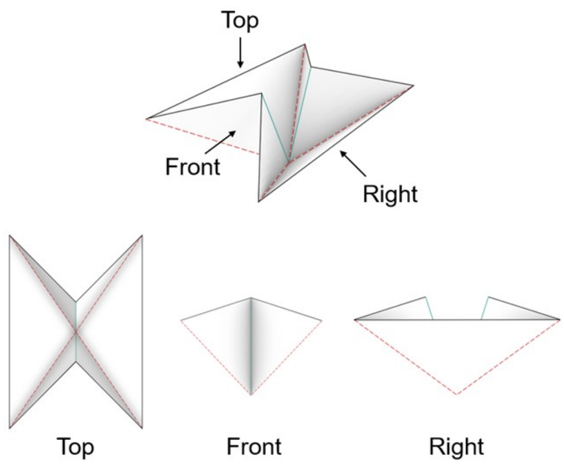


**Fig. S3.** The waterbomb origami pattern viewed from different directions.

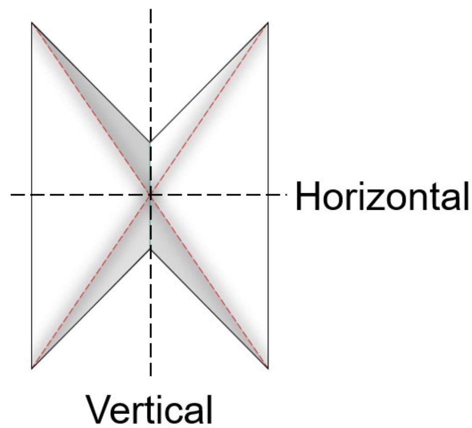


**Fig. S4.** Schematic showing the symmetry of the waterbomb pattern both vertically and horizontally.

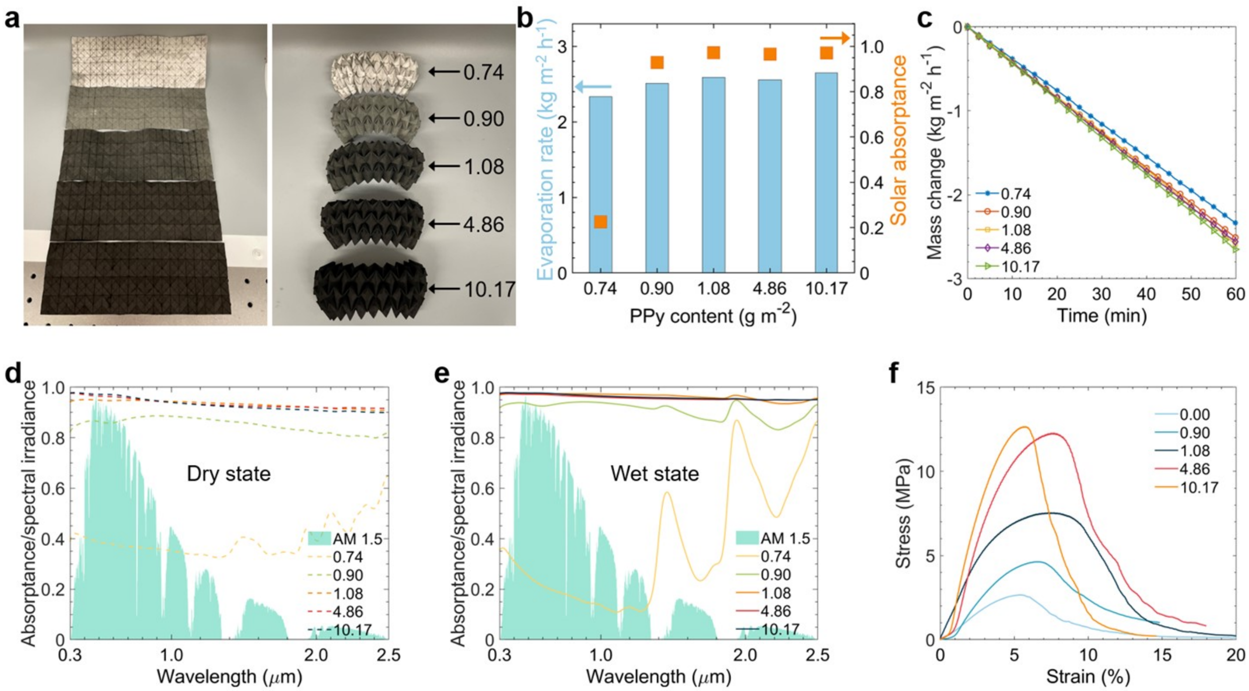


**Fig. S5.** (a) Photos of PPy-compounded cellulose paper with different PPy content in the fully expanded state (left) and folded state (right) in the dry state, respectively. (b) The evaporation rate (blue bar, left y-axis) and the solar absorptance (orange square, right y-axis) for the origami tower in the diameter of 40 mm with different PPy contents under one sun irradiation. (c) The mass changes of water with origami tower in the diameter of 40 mm with different PPy content under one sun irradiation. The solar absorptance spectra of the PPy-compounded cellulose paper with different PPy content in dry state (d) and in the wet state (e), respectively, displaying against the AM 1.5 spectral solar irradiance spectrum. (f) Tensile stress-strain curves of PPy-compounded cellulose paper with different PPy content in the wet state.

The PPy content in the composite sheet with a unit of (g $m^{-2}$), which demonstrates the mass of PPy component attached on the unit area of pristine cellulose paper. The PPy content can be expressed with the equation below:

$$PPy\ content = \frac{m_{black} - m_{white}}{A} = \frac{\Delta m}{A}$$

where $m_{black}$ is the mass of the dried black PPy-compounded cellulose paper with the unit of *g*, $m_{white}$ is the mass of the dried white pristine cellulose paper with the unit of *g*, $\Delta m$ is the mass of PPy component generated on the cellulose paper with the unit of *g*, and $A$ is the area of the cellulose paper with the unit of $m^2$.

As a photothermal material attaching on the exterior surface of the cellulose fibers, PPy is formed via the chemical polymerization process involving stirring pyrrole as the monomer and ammonium persulfate as the oxidant in an aqueous solution. In this work, the oxidation time for the composite sheet is 2 hours, and the averaged corresponding PPy content is 10.17 g $m^{-2}$ via the equation defined above. To further validate the effect of the PPy content on evaporation performance, the PPy-compounded cellulose papers with different PPy content are obtained by controlling the polymerization time, as shown in Figure S5. The values inserted in photo in the Figure S5a indicate the PPy content for each sheet. In the dry state, the composite sheet visually looks darker and darker with the increase of PPy content from almost white to ultra-black. But after absorbing water, as shown in Figure S5b, the composite sheet with PPy content of 1.08, 4.86, and 10.17 g $m^{-2}$ exhibit excellent overall light absorption around 97% across the solar spectrum from wavelength of 0.3 µm - 2.5 µm. Even for the composite sheet with PPy content of 0.90 g $m^{-2}$ in the appearance of light grey, its solar absorptance is close to 93% in the wet state, which still can be regarded as a good solar absorber. But when little PPy component is present in the composite paper (PPy content = 0.74 g $m^{-2}$), the solar absorptance drops significantly to 22%. Correspondingly, the evaporation rate for the origami tower in the diameter of 40 mm with different PPy content is tested indoor under one sun irradiation, and the results are shown in Figure S5b and Figure S5c. Except for the origami tower with PPy content of 0.74 g $m^{-2}$, other four origami towers display the consistently high evaporation rate although the one with 0.9 g $m^{-2}$ PPy content slightly lower than other three. Unexpectedly, the lowest evaporation rate of 2.3 kg $m^{-2}$ $h^{-1}$ is given by the origami tower with 0.74 g $m^{-2}$ PPy content which possesses the relatively low solar absorptance. The specific solar absorptance spectra of the PPy-compounded cellulose paper with different PPy content in the dry state and wet state are shown in Figure S5d and Figure S5e, respectively. Although the composite cellulose paper with the PPy content higher than 0.9 g $m^{-2}$ exhibit the consistent evaporation performance, they behave differently in mechanical property in wet state which demonstrates by the tensile stress-strain curves via the stretching test (Figure S5f). The PPy-compounded cellulose paper with the PPy content of 0.9 g $m^{-2}$ in the wet state presents the ultimate tensile strength and the fracture strain are 4.64 MPa and 6.5%, respectively. But when the PPy content of the composite paper increases to 4.86 g $m^{-2}$, its ultimate tensile strength and the fracture strain in the wet state are improved to 12.28 MPa and 7.7%, respectively, which indicating that the large PPy content is beneficial to enhance the mechanical strength of the PPy-compounded cellulose paper.

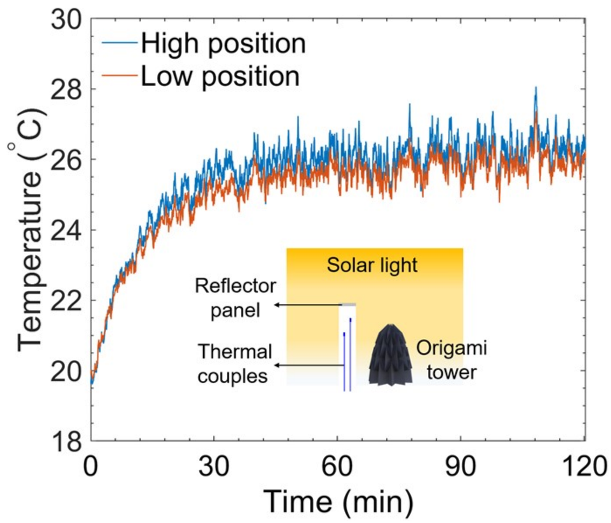


**Fig. S6.** Ambient temperature of the air below the light-reflecting panel relative to irradiation time under one sun irradiation. The inset schematically displays the setup used to measure the air temperature. There are two K-type thermal couples used to measure the ambient temperature around the origami tower, one is higher, and the other is lower. In order to eliminate the influence of direct sunlight on thermocouple temperature measurement, a light barrier is suspended over two thermal couples.


**Fig. S7.** Schematically showing the solar light provided by the solar simulator shines vertically on the evaporation device in the indoor evaporation test.

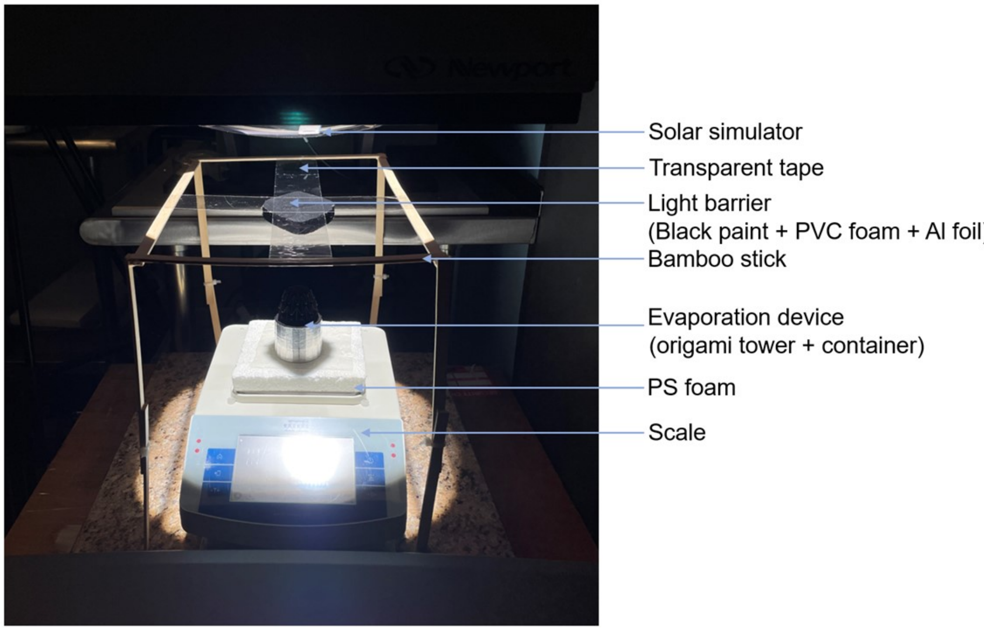


**Fig. S8.** Photo of the origami tower under diffusive light in water evaporation. Origami tower is placed on an electric scale which is connected to a laptop to record the real-time mass of the evaporation device (including the origami tower, water, and container). There is a piece of polystyrene (PS) foam covering the metal pan of the scale under the water container to prevent the conductive heat transfer from the scale to the water container under light illumination. To block the direct sunlight shining on the origami tower, a 7 mm thick polyvinyl chloride (PVC) foam with a diameter of 45 mm is suspended directly above the evaporation device fixed by the transparent tape as a light barrier, while the maximum diameter of the origami tower is 40 mm. PVC foam with closed pores has a very low thermal conductivity of 0.03 W $m^{-1}$ $K^{-1}$. The sun-facing side of the PVC foam is painted with a thin layer of black paint to absorb the sunlight, and the bottom side of the PVC foam, facing the origami tower, is covered with an Al foil tape. The Al foil shows a low thermal emittance which can minimize the thermal reemission from the bottom of the PVC foam to the origami tower. The solar simulator provides sunlight with intensity of 1 kW $m^{-2}$.

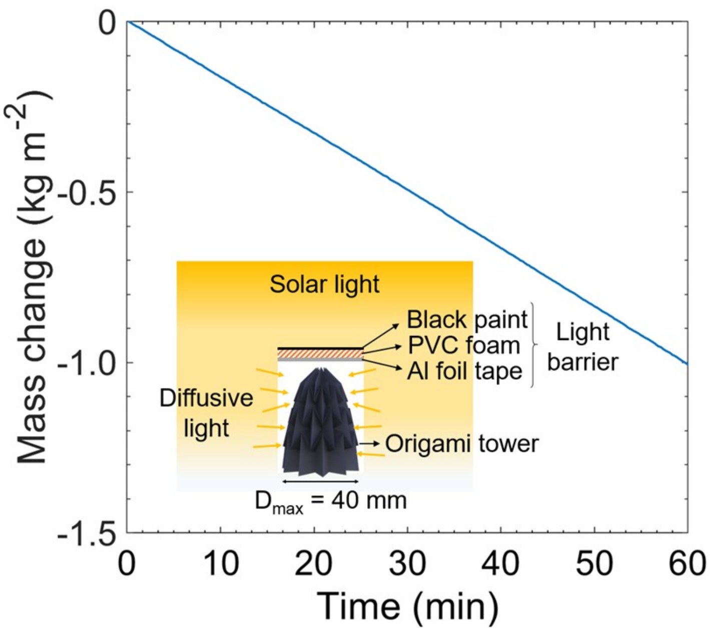


**Fig. S9.** Mass change of water with a maximum diameter of 40 mm under diffusive light.

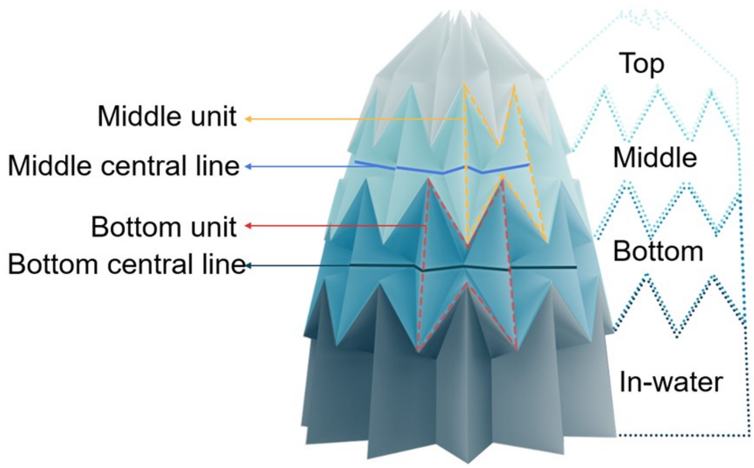


**Fig. S10.** Schematic illustration of the central lines of three adjoining waterbomb patterns and a single waterbomb pattern in the middle and bottom parts for an origami tower, respectively. The blue line represents the central lines in middle part. The black line represents the central lines in bottom part. The single waterbomb pattern in middle and bottom parts are highlighted by the yellow and red dashed curves, respectively.

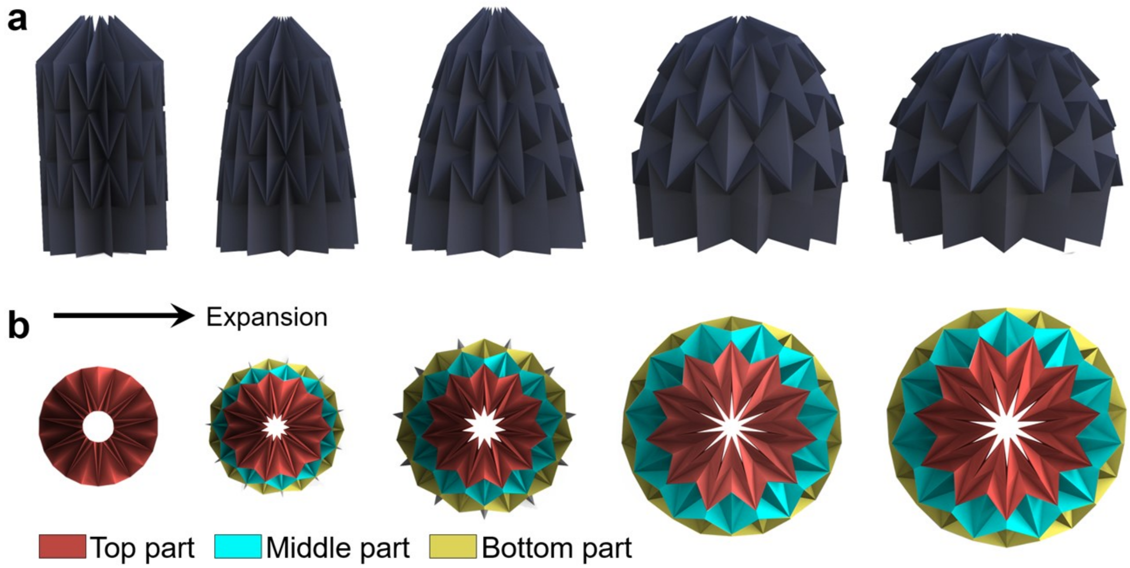


**Fig. S11.** Schematic representations of the expansion process (from left to right) of the convertible origami tower in the side view (a) and color-marked top view (b), respectively.

The convertible property and predictable deformability of the origami tower endow it with a capability to expand radially, accompanying with the relatively small shortening in the axial direction (Figure S11a). Due to the deformation of three-dimensional geometrical structure of the origami tower in the expansion process, the solar illumination situations over different parts of the tower vary because of its oblique angles. As shown in Figure S11b, the top, middle, and bottom parts of the origami tower are marked with different color in the top view at where it receives direct solar light. Obviously, in the expansion process with the increasing diameter, the origami tower with the larger diameter exposes more area by opening the waterbomb pattern up to receive more solar light, especially for the top and middle parts. When the diameter of the origami tower is larger than 50 mm which is almost completely inflated, the waterbomb patterns in the bottom part are approximately perpendicular to the bulk water surface without direct solar light exposure.

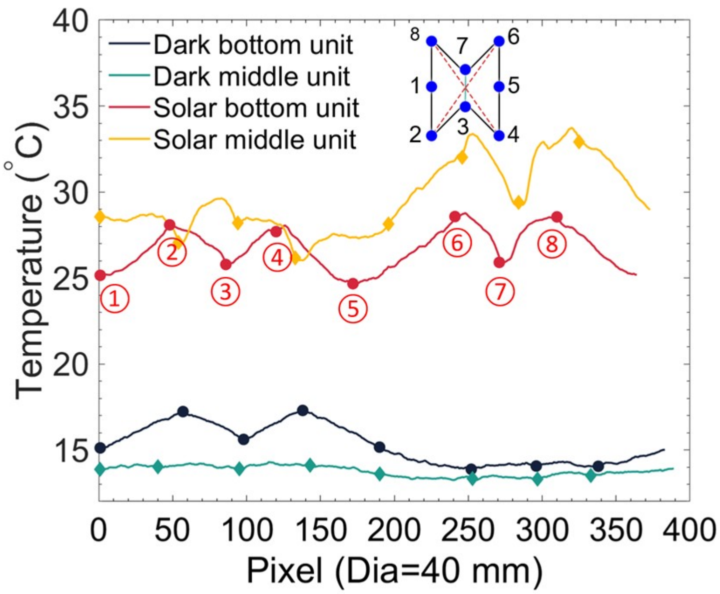


**Fig. S12.** Schematically showing the solid circles on the temperature curves correspond to the nodes in the inset.

Al foil tape Transparent tape

**Fig. S13.** The photographs of aluminum foil tape (left) and the transparent tape (right).

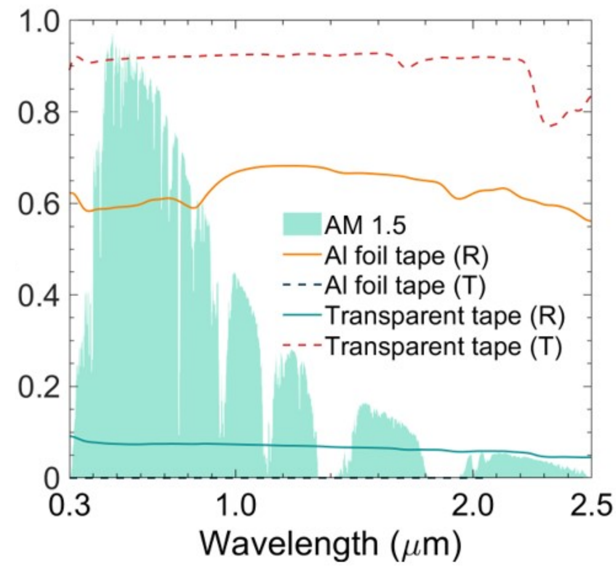


**Fig. S14.** The reflectance and transparence spectra of the Al foil tape and transparent tape against the normalized AM 1.5 spectral solar irradiance spectrum, respectively.

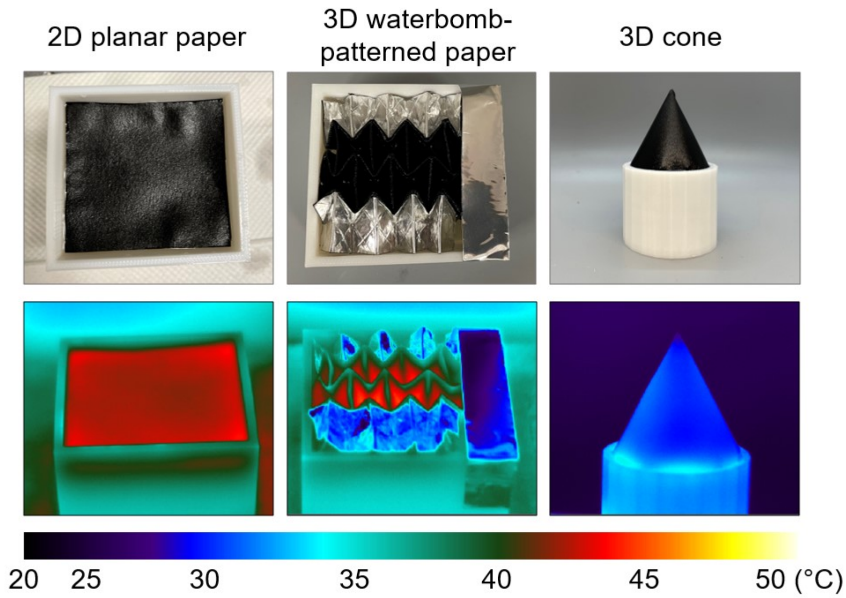


**Fig. S15.** The photographs of evaporation devices with 2D planar paper, 3D waterbomb-patterned paper, and 3D smooth cone, respectively (First row). The infrared images showing the temperature distribution of the 2D planar paper, 3D waterbomb-patterned paper, and 3D smooth cone working as an evaporator under one sun irradiation at the stable state.

2D planar paper in a dimension of 54 cm × 59 cm × 0.18 mm floats on water in a cuboid water container. The 3D waterbomb-patterned paper is comprised of 8 adjoining waterbomb patterns divided into two lines. The width of each unit of pattern is 13 mm. Other areas are sealed with impermeable Al foil tape which has high reflectivity for solar light. The 3D cone is in the dimension of 40 mm in diameter and 40 mm in height.

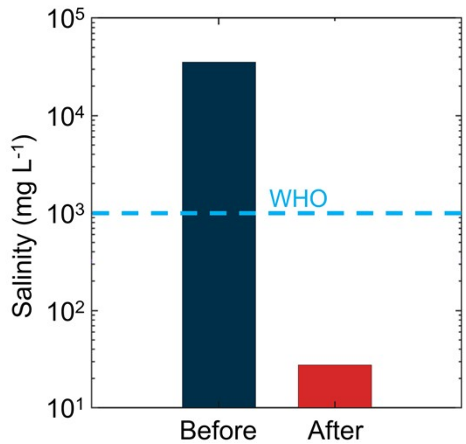


**Fig. S16.** Salinity of the water solution before and after desalination.

The freshwater water is collected evaporated via the origami tower with actual seawater to evaluate the salinity. The seawater collected from Revere Beach, Boston, US is applied as a raw water source. The Extech EC400 ExStik salinity meter is utilized to characterize the salinity of the seawater and collected freshwater sample. The salinity of water after desalination is dramatically reduced by approximately over three orders of magnitude and is below the drinking water standards defined by the World Health Organization (1‰), indicating the effective purification of the seawater.

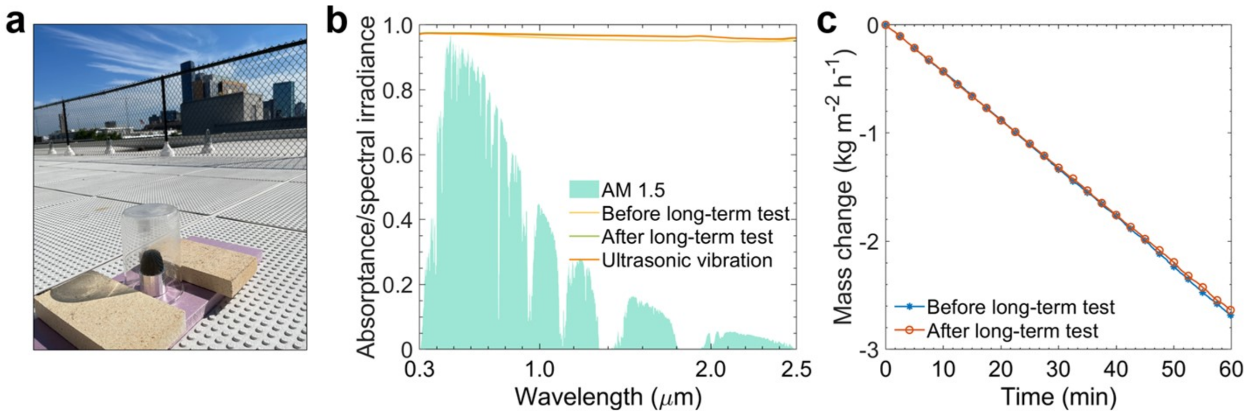


**Fig. S17.** (a) Photo of long-term outdoor test for the solar-driven evaporation with the origami tower. (b) The absorptance spectra of the wet PPy-compounded cellulose paper in the initial state, after 5-hour ultrasonic vibration, and after a 13-day long-term outdoor test, respectively. (c) The mass changes of water with the origami tower before and after the long-term outdoor evaporation test under one sun irradiation.

To further test the stability of the origami tower, a long-term outdoor evaporation test is conducted at the rooftop of Snell Engineering Center at Northeastern University, Boston, MA, USA from June 29 to July 11, 2022. Figure S17a shows the photo of outdoor test. The evaporation device is comprised of the origami tower with a diameter of 40 mm which is placed in a 3D printed water container filling with water. A large glass beaker with 10 cm in diameter and 15 cm in height covers the entire evaporation device placing on the rooftop under solar light for 13 days in a row. The solar absorptance spectra of the PPy-compounded cellulose paper before and after the long-term outdoor test are measured in Figure S17b. These two solar absorptance curves remain almost consistent even after prolonged solar exposure to the solar light, elucidating the spectrum stability of the photothermal materials attaching on the cellulose fibers. Furthermore, the PPy-compounded cellulose sheet was soaked in water under the ultrasonic vibration test for 60 minutes to valid its stability, and the corresponding solar spectrum of it after the vibration is also shown in Figure S17b, which is agreeing with other two curves. The evaporation ability of the origami tower after a long-term outdoor test was confirmed by the indoor experiment under one sun irradiation. Figure S17c represents the mass changes of water with the origami tower before and after the long-term test. The close evaporation performance indicates that the prolonged outdoor work did not obviously damage its evaporation ability, validating the stability of this evaporation device.

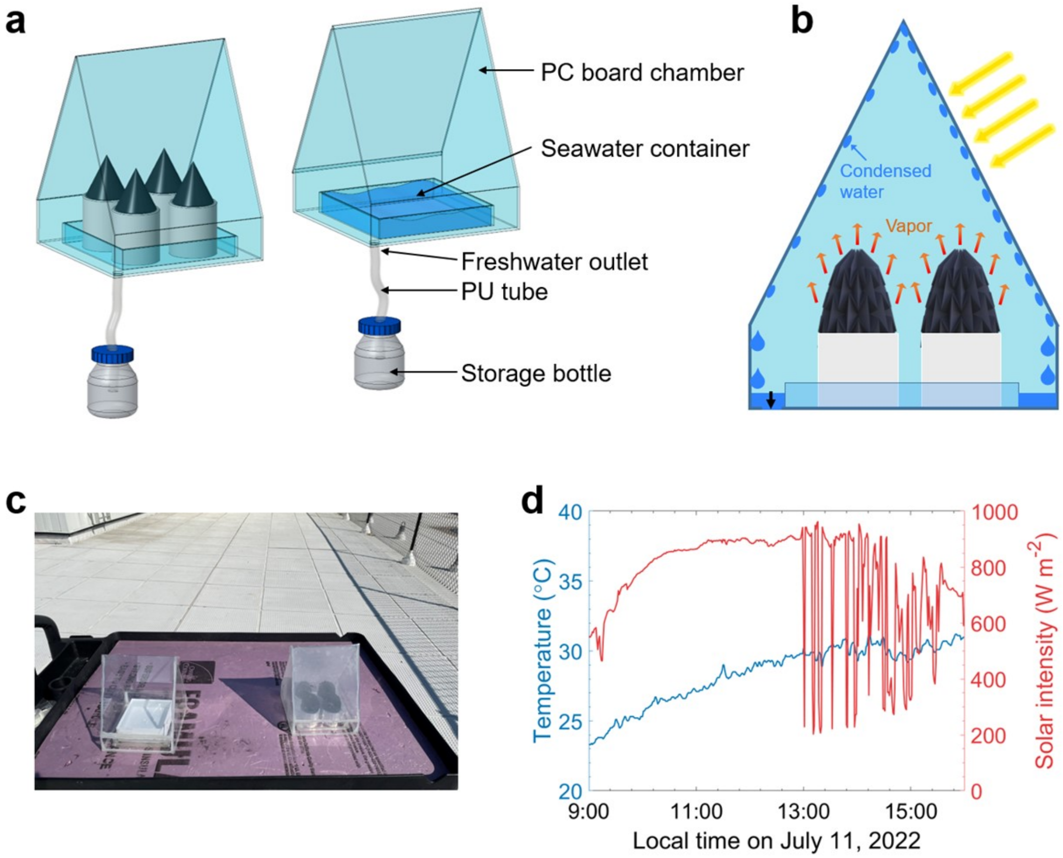


**Fig. S18.** Outdoor solar-driven desalination test. (a) Three-dimensional model of solar-driven desalination system with origami tower-based evaporator (left) and the control group without evaporator (right). (b) Schematic illustrating the mechanism of water evaporation and freshwater collection. (c) Photograph of the solar-driven desalination chambers which are placed on a utility cart. (d) Ambient temperature (solid blue curve) and solar intensity (solid red curve) variations during the outdoor desalination test recorded by the weather station near the evaporation device.

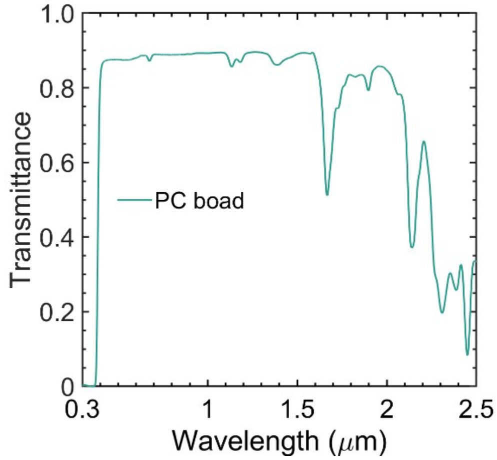


**Fig. S19.** Transmittance spectrum of a PC board over the solar wavelengths.

To validate the solar-driven desalination performance of the origami tower-based desalination system under natural sunlight, the outdoor test was run at the rooftop of Snell Engineering Center at Northeastern University, Boston, MA, USA on July 11, 2022. The solar desalination system is composed of a sealed condensation chamber and four origami tower with a diameter of 40 mm which is placed in the water container individually (Figure S18a). The condensation chamber covers the top of the evaporation device to capture the evaporated vapor. Besides, the chamber is made of polycarbonate (PC) board with a thickness of 0.8 mm and an overall transmittance of 83% (Figure S19) in the range of solar wavelengths (0.3 μm - 2.5 μm). The PC board is transparent in the solar spectrum to allow the solar irradiance to reach the origami tower. The generated freshwater flows to the water storage bottle through a polyurethane (PU) tube. The generated water vapor from the origami tower condensates on the inner wall of the PC board, and then, the condensed water droplets flow downward along the wall to the water collection tank and finally to the water storage bottle (Figure S18b).

The experimental group encapsulated the origami tower-based evaporation device inside, while only the water is stored inside the water container (9 cm × 9 cm × 5 cm) as a control group without any photothermal materials. Both the experimental and the control groups of the solar desalination system are placed on the polystyrene (PS) foam between the bottom of the two prototypes and the utility cart (Figure S18c). The PS foam has a low thermal conductivity of 0.03 W $m^{-1}$ $K^{-1}$ and it can effectively block the heat transfer between the PC prototype chambers and the black utility cart since the cart can be heated up to a high temperature under sunlight in the summer. The weather station records the data of the solar intensity and ambient temperature (Figure S18d). The average ambient temperature and solar intensity are 27°C and 684 W $m^{-2}$, respectively, during the experimental period from 9:00 to 16:00. At the end of the outdoor experiment, 42.95 g of freshwater is collected in the storage bottle from the prototype with origami tower evaporator, while the control group only collects 9.07 g of water. The freshwater collection ability of the origami tower-based evaporation device group during the test is 8.55 kg $m^{-2}$, while the control group is only 1.12 kg $m^{-2}$. It is worth noting that the weight of the collected freshwater is less than that of the condensed water. The obvious difference between the experimental and control group validate the good performance of the origami tower-based evaporation device.

**Note S2**

**The evaporation tests in dark environment**

The evaporation tests for the origami tower with different diameters are conducted in a dark room with temperature and humidity maintained at 19 - 20ºC and 30 - 32%, respectively. The initial temperature of water is around 20ºC. Initially, the mass of four evaporation devices with origami towers in diameters of 30 mm, 40 mm, 50 mm, and 60 mm, respectively, are weighted individually, then, put them in the dark room. After 3 hours of water evaporation in dark, the weight of each evaporation device is weighted again to get the mass loss of water.